Economical design of buried concrete pipes subjected to UK standard traffic loading

Alzabeebee, Saif; Chapman, David; Faramarzi, Asaad

DOI:
10.1680/jstbu.17.00035

Paper Submitted: 07/03/2017

Paper Revised: 09/10/2017

Paper title: Economical design of buried concrete pipes subjected to UK standard traffic loading

Authors:

Saif Alzabeebee (Corresponding author) (BSc, MSc, PhD, AMASCE)

Department of Civil Engineering, School of Engineering, University of Birmingham, Birmingham, B15 2TT, UK

ORCID: 0000-0001-9685-5641

E-mail: Saif.Alzabeebee@gmail.com

David Chapman (BSc (Hons), DIS, PhD, CEng, MICE, FHEA)

Department of Civil Engineering, School of Engineering, University of Birmingham, Birmingham, B15 2TT, UK

Asaad Faramarzi (BSc, MSc, PhD, FHEA)

Department of Civil Engineering, School of Engineering, University of Birmingham, Birmingham, B15 2TT, UK

Abstract

The British Standard (BS) uses the indirect design method to design buried concrete pipes under the effect of traffic load, where in this method the laboratory capacity of the pipe is obtained and linked to the field capacity using an empirical factor called the bedding factor. However, the BS design bedding factors have not been rigorously tested. This paper therefore presents a rigorous analysis of the response of buried pipes under the BS traffic loading requirements and tests the robustness of the BS design bedding factors using a validated finite element model. It was found that the BS bedding factors are overly conservative with a ratio of calculated values to the design bedding factors ranging from 1.63 to 4.92. This over conservatism is due to the oversimplification in the BS methodology for calculating the force applied to the pipe. Therefore, new bedding factors have been proposed utilising the evolutionary polynomial regression analysis technique. These bedding factors implicitly account for the error due to the oversimplification in the design force calculation. Hence, more economical and robust designs can be achieved by using the new bedding factors.

Keywords: pipes and pipelines; design methods and aids; structures and design.

Abbreviations

BF	bedding factor
T_w (m)	width of the trench
D_{out} (m)	outside diameter of the pipe
SW95	well-graded sand with a degree of compaction of 95% of the Standard Proctor test
SW90	well-graded sand with a degree of compaction of 90% of the Standard Proctor test
ML90	sandy silt with a degree of compaction of 90% of the Standard Proctor test
ML49	sandy silt with a degree of compaction of 49% of the Standard Proctor test
E (kPa)	modulus of elasticity
υ	Poisson's ratio
D (m)	inside diameter of the pipe
t (m)	pipe wall thickness
γ (kN/m^3)	unit weight of the soil
c' (kPa)	cohesion of the soil
ϕ'	angle of internal friction of the soil
K	modulus number
R_f	failure ratio
n	modulus exponent
H (m)	backfill height
M_{lab} (kN.m/m)	maximum bending moment in the laboratory condition
W_t (kN/m)	total force applied on the pipe
$W_{backfill}$ (kN/m)	backfill soil weight force applied on the pipe
$W_{traffic}$ (kN/m)	traffic load force applied on the pipe
r (m)	radius of the pipe measured to the centre of the pipe wall
C_c	soil load factor for the case of wide trench condition
C_d	soil load factor for the case of a narrow trench condition
M(kN.m/m)	maximum field bending moment predicted from the finite element modelling
CD	coefficient of determination

1. Introduction

Buried concrete pipelines are vital to maintain modern life by providing an economical and convenient way to transport water and sewage (Mohamed et al., 2014; Rakitin and Xu, 2014). Buried concrete pipes are commonly designed using the indirect design method according to the British Standard (BS) (BSI, 2010). The indirect design method is based on testing the pipe in the laboratory using a three-edge bearing test, where in this test the pipe is supported in the invert zone only and subjected to a line load at the crown. The pipe should resist the applied load without exceeding a crack width limit of 0.254 mm (MacDougall et al., 2016). The maximum applied load in the three-edge bearing test is equal to the maximum force that the pipe is expected to experience in the field multiplied by an appropriate factor of safety (FS) divided by an empirical factor called the bedding factor (BF) (Alzabeebee et al., 2018). This bedding factor is usually used because the support condition for the pipe in the field is different from that in the three-edge bearing test. Hence, the bedding factor is key in the design of concrete pipes (Alzabeebee et al., 2017b). Despite the importance of this factor, no study has investigated the robustness of the current bedding factor values adopted in the BS for the case of buried pipes under the BS traffic loads (two axles with an axle load of 450 kN (BSI, 2010)). Furthermore, there are limited studies on the bedding factor for buried concrete pipes under the AASHTO truck loads (one axle load with a nominal axle load of 142 kN) (MacDougall et al., 2016; Petersen et al., 2010), where these studies have shown that the current bedding factor values adopted in the AASHTO standard are conservative. MacDougall et al., (2016) investigated the bedding factor experimentally by testing the pipe in the laboratory. Petersen et al., (2010) investigated the bedding factor numerically by dividing the maximum positive bending moment developed in the pipe

wall in the three-edge bearing test (calculated from a verified closed form solution) by the maximum positive bending moment developed in the buried pipe wall predicted using the finite element modelling. However, these studies cannot be used to test and improve the current BS bedding factors because of the significant difference of the load configuration and the maximum axle load between the BS design truck and the AASHTO truck considered in these studies. Other studies have also been conducted on concrete pipes under traffic load, but these studies did not focus on the accuracy of the design bedding factors and only considered the American or Canadian standard traffic loading (Ban et al., 2013; Lay and Brachman, 2014; Nehdi et al., 2016).

Furthermore, a review of previous studies has shown differences in opinion with respect to the recommended backfill height limit for the effect of the traffic load. For example, the American Concrete Pipe Association (ACPA) (2011) recommended ignoring the effect of the traffic load of an AASHTO HS-20 truck (one axle with a nominal axle load of 142 kN) when the backfill height above the pipe is equal to or greater than 3 m. However, Rakitin and Xu (2014) found from a centrifuge study that the traffic load affects the bending moment in the concrete pipe wall even for a backfill height of 4 m. Rakitin and Xu (2014) justified the difference between their results and the recommended ACPA backfill height limit due to the higher axle load used in their experiment (567 kN), which was significantly higher than the HS-20 axle load (142 kN). However, only one wheel was used in the experiment with a maximum wheel stress of 468 kPa, which is lower than the nominal wheel stress of the HS-20 truck (568 kPa). On the other hand, the BS (BSI, 2010) does not recommend a backfill height limit for the effect of the traffic load. In addition, the previous studies did not consider the effect of the pipe wall thickness on the pipe

response under traffic load, although changing the pipe wall thickness significantly affects the pipe stiffness (Peterson et al., 2010), which will change the percentage of load attracted by the pipe based on the arching theory (Moore 2001, Kang et al., 2007).

The present study therefore presents an in-depth analysis of the effect of the BS traffic load on the response of buried concrete pipes. The study is divided into two parts. The first part aims to identify the key parameters affecting the bending moment in the pipe wall under the traffic load by conducting a parametric study investigating the effect of the backfill height, pipe diameter, installation quality and pipe wall thickness. These parameters are the key parameters affecting the pipe response and were considered based on an intensive literature review done during the early stages of this research. The second part focuses on investigating the robustness of the current bedding factor values adopted in the BS by utilising the maximum bending moment obtained from the finite element modelling.

2. Current bedding factor values

According to the BS (BSI, 2010), the selection of the bedding factor is mainly dependent on the installation condition, where improving the installation quality increases the bedding factor value and vice versa. Currently, there are two installation types: concrete bedding and granular bedding or natural base. These installation types are divided into classes based on the support condition. However, only the second type is considered in this study because it is more practical. Table 1 shows the installation classes and the corresponding bedding factor values for the second type.

Table 1: Installation classes of granular bedding or natural base installation according to the British Standard (Young and O'Reilly, 1987; BSI, 2010; Alzabeebee et al., 2018)

Installation configuration	Installation class	Bedding factor value
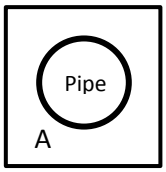	S	2.2
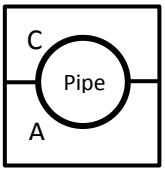	B	1.9 to 2.3
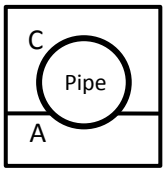	F	1.5 to 1.9
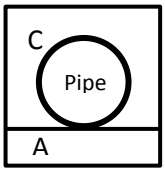	N	1.1 to 1.3
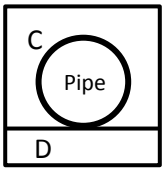	DD	1.1 to 1.3

Note: A, single size granular material; C, backfill soil free of tree roots, frozen soil, clay lamps, stones larger than 40 mm or any material larger than 75 mm; D, natural soil

3. Numerical modelling details

The three-dimensional finite element model used in this study was developed using MIDAS GTS/NX (2015), a commercial three-dimensional finite element software. This model was validated using laboratory and full scale test results from the literature. Details of the numerical model validation can be found in Alzabeebee et al. (2017a) and Alzabeebee et al. (2018). The length, width and height of the numerical model were equal to 15 m, 12 m and 10 m, respectively. The trench and the surrounding soil were modelled using four noded tetrahedron solid elements and the pipe was modelled using three noded triangular shell elements. The thin shell theory has been considered (i.e. using shell elements to model the pipe) to simulate the case of a conservative analysis, which is always preferred in practice, as the thin shell theory predicts a higher bending moment at the crown of the pipe than the thick ring theory (Moore et al., 2014).

Fine mesh with an average element size of 0.15 m was used to model the pipe and the trench, while coarse mesh with an average element size of 0.5 m was used to model the surrounding soil. The bedding layer was assumed to have a thickness of 10 cm. The BS main highway (‘main road’) traffic load was considered because this loading configuration simulates the worst case scenario (BSI, 2010). This loading configuration consists of two axles with four wheels in each axle. The total single wheel load is equal to 112.5 kN. The wheel load area is assumed to have a length of 0.5 m and a width of 0.25 m (Petersen et al., 2010; Kang et al., 2013a; Kang et al., 2014). The case of a truck travelling perpendicular to the pipe direction with the first

axle being directly above the pipe was considered in the modelling, as shown in Figure 1. This loading position was considered because it represents the worst case scenario (Alzabeebee et al., 2017a). The backfill soil, bedding soil and in-situ soil were modelled using the hyperbolic Duncan-Chang soil model (Duncan and Chang, 1970). This model was used because it is capable of simulating the behaviour of the soil around buried culverts with good accuracy, hence a more accurate representation to the problem could be achieved with this model (Dhar et al. 2004; Kim and Yoo, 2005; Kang et al., 2007; Kang et al., 2008a, b; Kang et al., 2013a, b; Turan et al., 2013; Kang et al. 2014; Katona, 2017). A linear elastic model was used to model the concrete pipe. The finite element mesh used in the analysis is shown in Figure 2. Four steps were performed in the finite element analyses similar to that used by other researchers (Allard and El Naggar 2016; El Naggar et al., 2015; Mehrjardi et al., 2015; Petersen et al., 2010).

Step 1: the vertical and horizontal stresses for the native soil were calculated. A coefficient of lateral earth pressure of 1.0 was used in the calculation.

Step2: the simulation of trench excavation was conducted by removing the soil elements in steps. The width of the trench (T_w) has been estimated based on the outside diameter of the pipe (D_{out}) using Equation 1 (Arockiasamy et al., 2006).

$$T_w = 1.5D_{out} + 0.3 \quad (1)$$

Step 3: the pipe and the trench soil were added in steps. The lateral earth pressure coefficient for the compacted soil was assumed to be 1 (Brown and Selig, 1991).

Step 4: the main road British Standard load was applied with a total number of 25 equal steps.

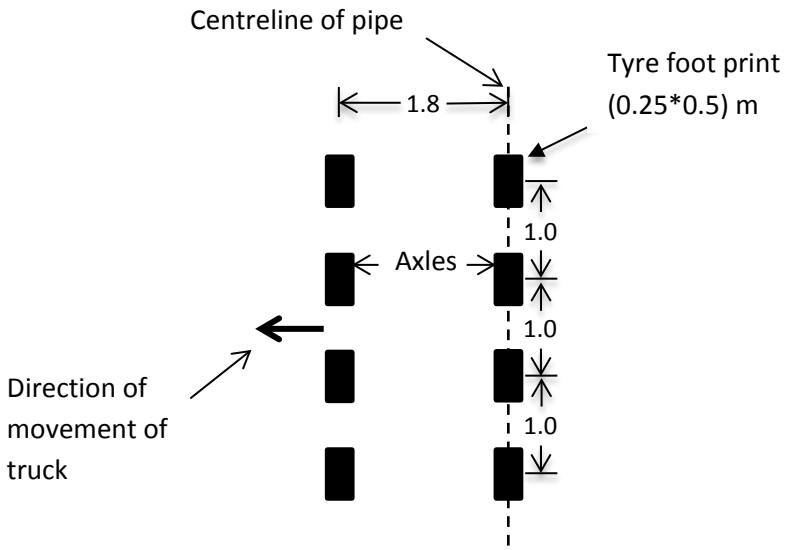

Figure 1: The British Standard main highway (‘main road’) loading configuration (BSI, 2010)

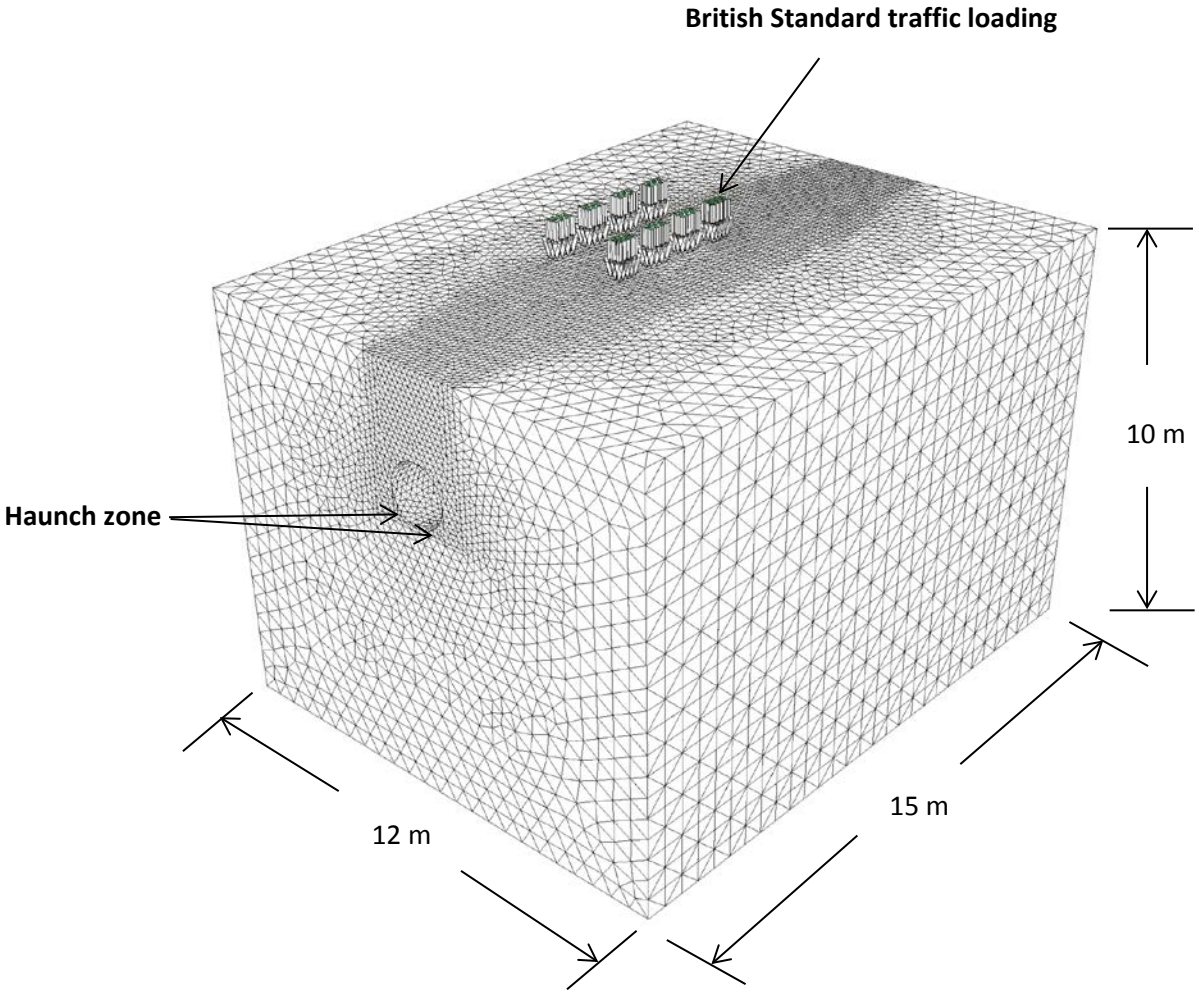

Figure 2: The finite element mesh used

4. Parametric study

A parametric study has been conducted to thoroughly investigate the effect of the BS traffic load on the bending moment developed in the buried concrete pipe wall, and hence enable a comprehensive understanding of the problem. The effect of pipe wall thickness, pipe diameter, backfill height and support condition have been considered in these analyses. Table 2 shows the diameters and the wall thicknesses considered in the analysis. A minimum backfill height of 1.0 m has been considered because it is the minimum backfill height allowed in the UK for the buried pipe under the main road traffic load (HA, 2001). The quality of the installation has been investigated by changing the soil in the haunch zone (the haunch zone is shown in Figure 2). Four

different installation conditions have been investigated covering the range of very good quality installation to a poor quality installation. The soils considered were SW95 (gravelly sand with a compaction degree of 95% according to the standard Proctor test) (to simulate a very good quality installation), SW90 (to simulate a good quality installation), ML90 (sandy silt with a degree of compaction of 90% according to the standard Proctor test) (to simulate a reasonable quality installation) and ML49 (to simulate a poor quality installation). The backfill soil above the pipe was simulated with the SW90 soil in all of the cases, while the surrounding soil was assumed to be stiffer than the backfill soil (Alzabeebee et al., 2017a). Furthermore, the bedding soil was simulated using the SW90 soil. The bedding soil was simulated with a well compacted soil to investigate the worst case scenario of a pipe directly installed on a stiff soil. The hyperbolic soil model parameters of these soils were taken from the literature (Boscardin et al., 1990) and are shown in Table 3. The modulus of elasticity (E) and the Poisson ratio (υ) of the concrete pipe were taken as 24,856 MPa and 0.2, respectively (Petersen et al., 2010). The following subsections discuss the results of this parametric study.

Table 2: Pipes diameters and wall thicknesses (Petersen et al., 2010)

Inside diameter (D) (m)	Wall thickness (t) (m)
0.3	0.051
0.6	0.076
1.2	0.127
2.4	0.229

Table 3: Material properties used in the parametric finite element analysis (Boscardin et al., 1990)

Property	SW95*	SW90*	ML90*	ML49*	Natural soil**
γ (kN/m3)	22.07	20.99	18.84	10.40	21
υ	0.3	0.3	0.3	0.3	0.3
c'(kPa)	1	1	24	1	30
ϕ'(°)	48	42	32	23	36
K	950	640	200	16	1500
Rf	0.7	0.75	0.89	0.55	0.9
n	0.6	0.43	0.26	0.95	0.65

* taken from Boscardin et al., (1990)

** assumed values

4.1. Effect of backfill height and pipe diameter

The bending moment due to the soil weight only and total load (combined soil weight and traffic load) have been investigated in this section. This was undertaken to study the reduction in the effect of the traffic load as the backfill height (H) increases for all of the considered diameters, and also to find the backfill height limit for the effect of the traffic load.

Figure 3 shows the bending moment due to the soil weight only and the total load for a pipe with an inside diameter of 0.3 m. It can be clearly seen that the presence of the traffic load significantly increases the bending moment in the pipe wall. However, the effect of the traffic load considerably decreases as the backfill height increases, where the percentage increase in the maximum bending moment due to traffic load

is 353% for a backfill height of 1 m and decreases to 22% for a backfill height of 2.5 m. It can also be seen that the traffic load did not affect the maximum bending moment for a pipe buried with a backfill height of 3.0 m.

Figures 4, 5 and 6 show the effect of the traffic load on the bending moment for pipes with an inside diameter of 0.6 m, 1.2 m and 2.4 m, respectively. Generally, these figures show a similar trend to that shown in Figure 3, where the traffic load increases the bending moment in the pipe wall. However, it can be clearly seen that increasing the diameter of the pipe decreases the influence of the traffic load. For a backfill height of 1 m, the percentage increase in the bending moment is 205%, 119% and 12% for pipes with an inside diameter of 0.6 m, 1.2 m and 2.4 m, respectively. Importantly, Figures 5 shows that the influence of the traffic load becomes very small at a backfill height of 2.5 m, where the percentage increase is less than 7%. Furthermore, Figure 6 shows that the traffic load has no effect on the maximum bending moment for a 2.4 m pipe with a backfill height of 1.5 m. This behaviour is different from that observed for pipes with diameters of 0.3 m, 0.6 m and 1.2 m (Figures 3, 4 and 5). This is due to the insignificant effect of the traffic load on the soil pressure developed at the invert of the 2.4 m pipe with a backfill height of 1.5 m as shown in Figure 7 when compared with the other diameters. Figure 7d shows that the mean soil pressure at the invert of the 2.4 m pipe does not increase due to the application of the traffic load, which is different from other diameters shown in Figures 7a, b and c. In addition, the initial soil pressure at the invert of the 2.4 m pipe (due to soil weight only) is higher than the crown soil pressure even after the application of the traffic load. Therefore, there was no increase in the maximum bending moment. These results are in general agreement with the ACPA recommendation on the influence of traffic load, where the ACPA suggests that the

traffic load is not significant for a backfill height equal to or greater than 3.0 m (ACPA, 2011). However, the present study has shown that although the ACPA recommendation is valid, it is conservative for large diameter pipes, where the effect of the traffic load becomes insignificant when the backfill height is equal to or greater 1.5 m for the 2.4 diameter pipe. Therefore, the BS should include a backfill height limit to the influence of traffic load depending on the pipe diameter.

Finally, comparing the results of Figures 3, 4, 5 and 6 shows that increasing the diameter of the pipe increases the bending moment at the shoulder, springline and invert of the pipe. This is due to the increase in backfill height above the pipe in these zones as the diameter increases, which means that the soil weight above these locations will increase. Hence, leading to a larger induced bending moment.

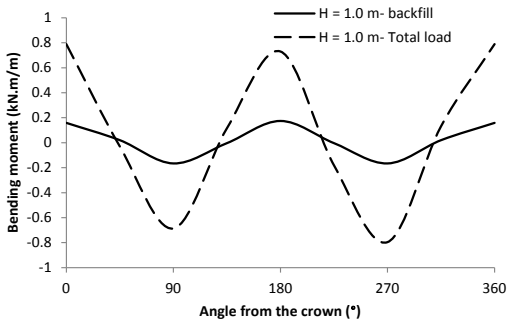

(a)

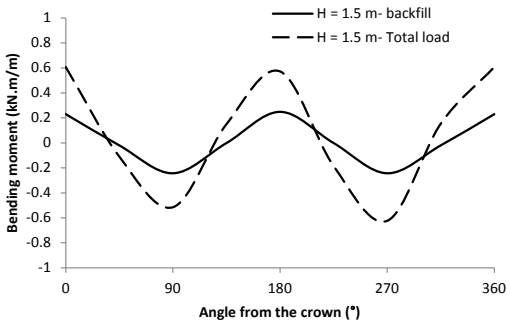

(b)

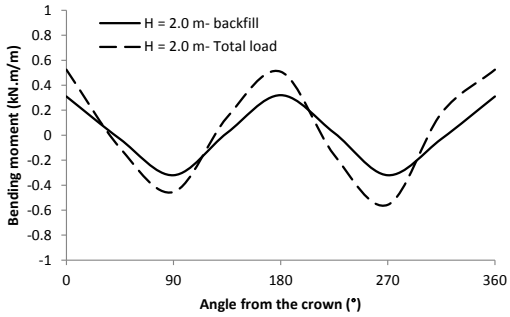

(c)

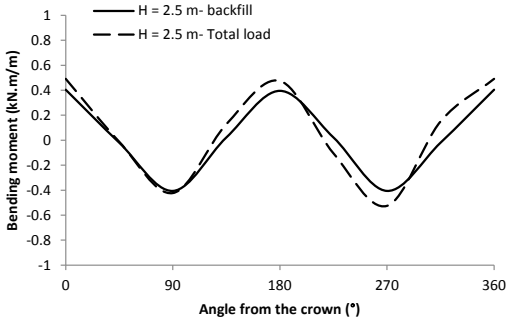

(d)

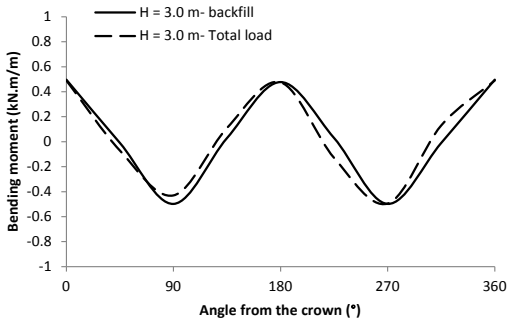

(e)

Figure 3: Bending moment around a pipe with an inside diameter of 0.3 m for different backfill heights: (a) H = 1.0 m; (b) H = 1.5 m; (c) H = 2.0 m; (d) H = 2.5 m (e) H = 3.0 m

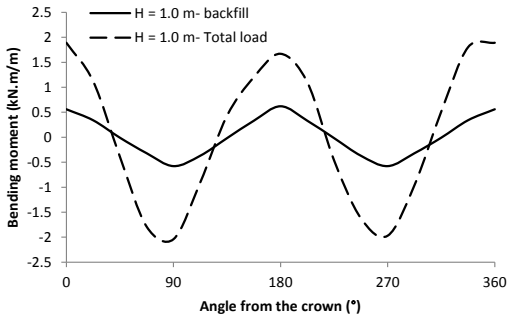

(a)

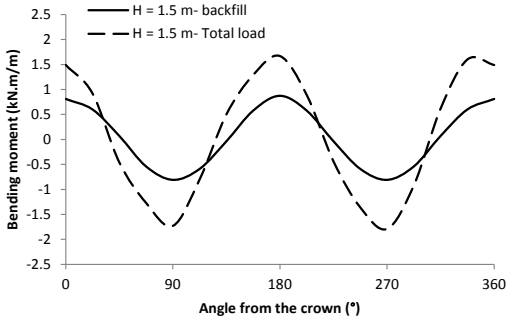

(b)

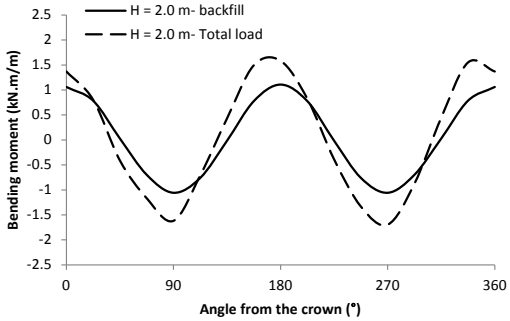

(c)

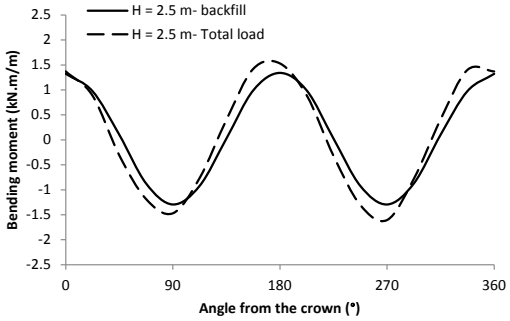

(d)

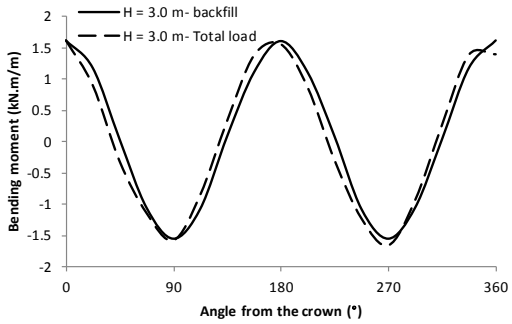

(e)

Figure 4: Bending moment around a pipe with an inside diameter of 0.6 m for different backfill heights: (a) H = 1.0 m; (b) H = 1.5 m; (c) H = 2.0 m; (d) H = 2.5 m (e) H = 3.0 m

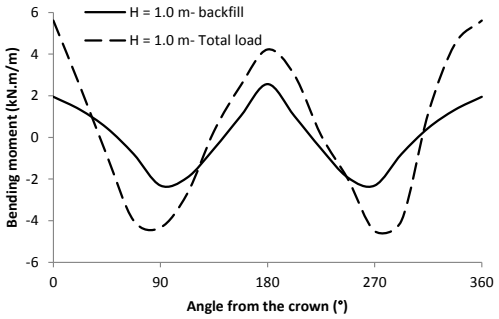

(a)

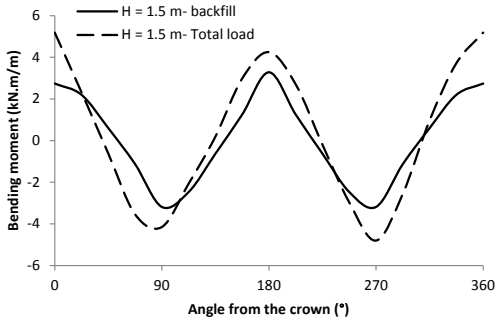

(b)

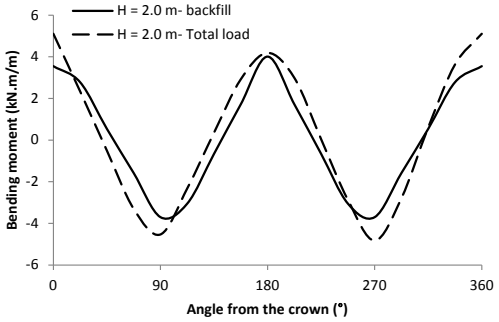

(c)

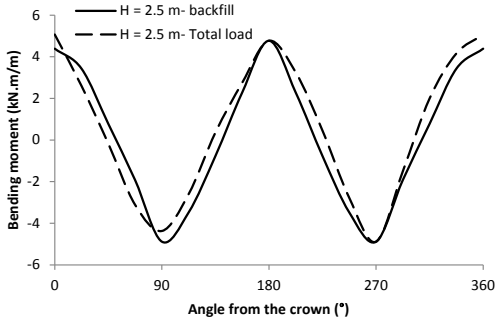

(d)

Figure 5: Bending moment around a pipe with an inside diameter of 1.2 m for different backfill heights: (a) H = 1.0 m; (b) H = 1.5 m; (c) H = 2.0 m; (d) H = 2.5 m

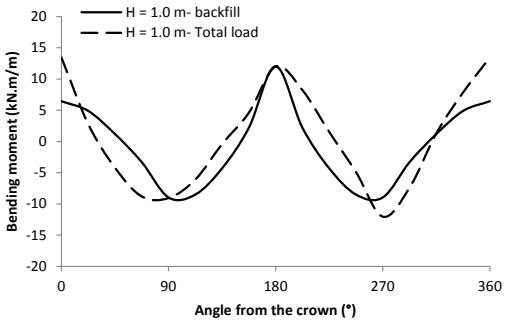

(a)

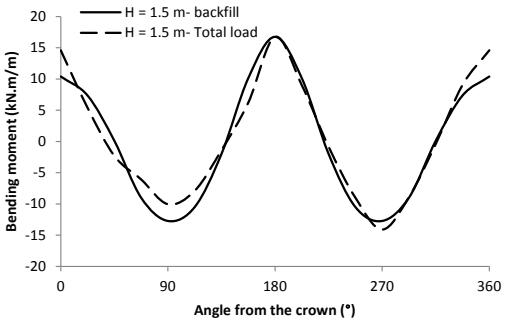

(b)

Figure 6: Bending moment around a pipe with an inside diameter of 2.4 m for different backfill heights: (a) H = 1.0 m; (b) H = 1.5 m

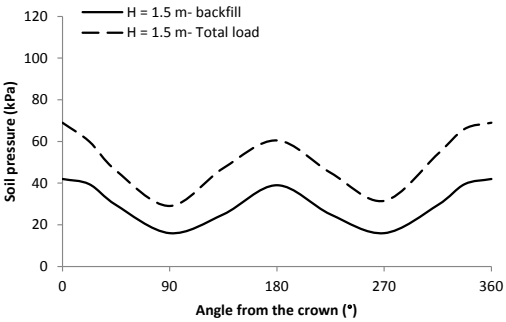

(a)

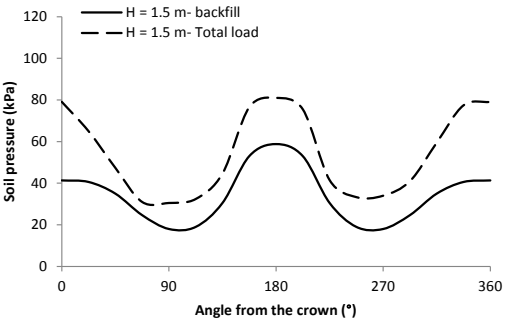

(b)

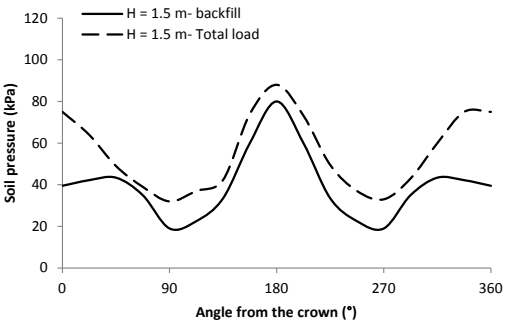

(c)

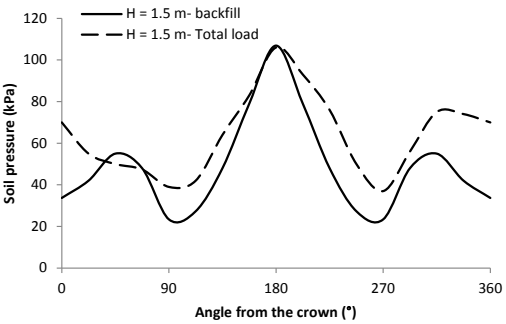

(d)

Figure 7: Mean soil pressure around the pipe: (a) D = 0.3 m; (b) D = 0.6 m; (c) D = 1.2 m; (d) D = 2.4 m

4.2. Effect of soil support (installation type)

The effect of the installation quality has been investigated by changing the soil type at the haunch zone. This has been considered because changing the quality of the haunch soil affects the soil pressure developed at the invert zone (Pettibone and Howard, 1967; Wang et al., 2006; Alzabeebee et al., 2016). Hence, this is expected to impact the induced bending moment in the pipe wall.

Figure 8 shows the effect of the installation quality on the induced bending moment for a pipe with an inside diameter of 0.3 m and a backfill height of 1.0 m under the total load. It can be seen from this Figure that the bending moment does not significantly increase when the haunch soil changes from SW95 (very good installation) to SW90 (good installation) or ML90 (reasonable installation), where the percentage increase is equal to 0.21% and 4%, respectively. The Figure also shows that as expected, changing the haunch soil from SW95 (very good installation) to ML49 (poor installation) noticeably increases the bending moment (percentage increase 36%) and changes the zone of the maximum bending moment from the crown to the invert of the pipe. It can also be seen that changing the installation quality does not significantly impact the bending moment developed at the crown or the springline.

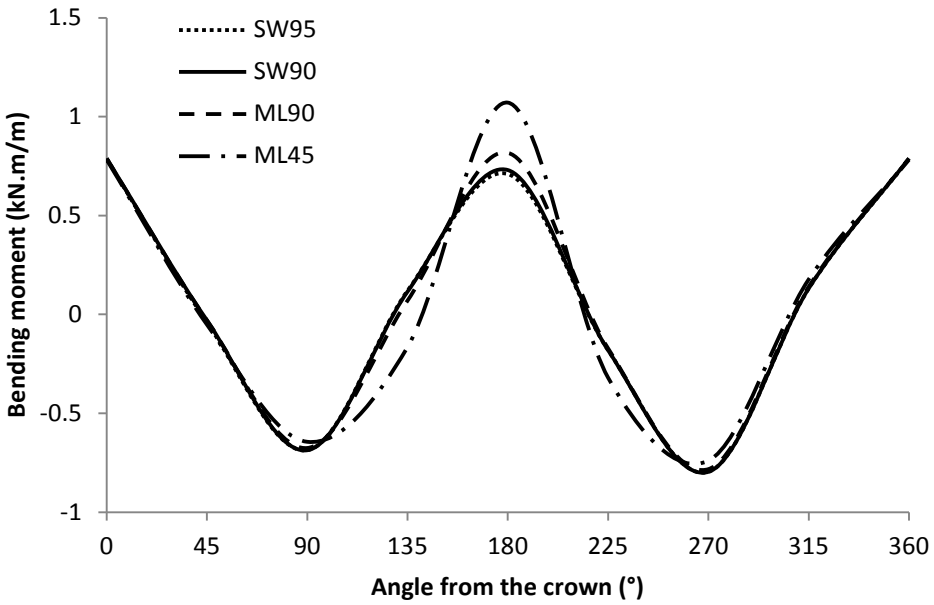

Figure 8: Effect of installation quality on the bending moment of a pipe with an inside diameter of 0.3 m and a backfill height of 1.0 m

4.3. Effect of pipe wall thickness

To investigate the effect of the pipe wall thickness, additional models were considered with two thicknesses: one was equal to half of the original thicknesses shown in Table 2 and the second was double of the original thicknesses. This was done for all of the pipes with all of the considered backfill heights. The aim was to study the impact of the pipe wall thickness on the bending moment developed in the pipe wall and quantify the percentage change in the bending moment. Figure 9 shows the effect of the pipe wall thickness on the bending moment due to the total load on a pipe with an inside diameter of 1.2 m and a backfill height of 1.0 m. It can be clearly seen that the bending moment is significantly affected by changing the pipe wall thickness, where decreasing the pipe thickness by half decreases the maximum bending moment by 48%, while doubling the pipe thickness increases the bending moment by 36%. This is due to an increase in soil pressure attracted by the

pipe as the stiffness increases due to the increase in the pipe thickness (and the opposite is also true, i.e. the soil pressure reduces when the pipe stiffness reduces due to a reduction in pipe thickness), and is explained by soil arching theory (Moore, 2001).

From this parametric study it can be concluded that the bending moment induced in the pipe wall due to the traffic loading, for the pipe diameters considered in this study, is affected by the backfill height (up to 2.5 m), the installation condition and the pipe wall thickness. Hence, all of these parameters should be considered when testing and improving the current design bedding factors. This is because the bedding factor is dependent on the bending moment as discussed earlier in the introduction (Young and O'Reilly, 1987; Petersen et al., 2010). The next section discusses the bedding factor and the robustness of the BS bedding factors.

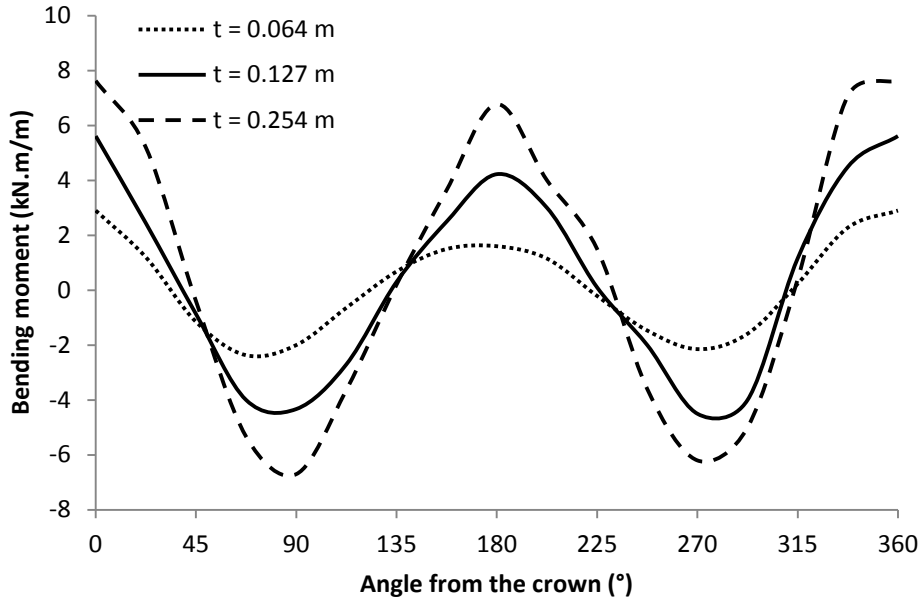

Figure 9: Effect of pipe wall thickness on the induced bending moment in the pipe wall for a pipe with an inside diameter of 1.2 m and a backfill height of 1.0 m under the total load

5. Bedding factor

The maximum bending moment obtained from the finite element modelling for each case was used to calculate the bedding factor. As the bedding factor links the laboratory capacity to the field capacity of the pipe, it can be obtained by taking the ratio of the maximum positive bending moment in the laboratory condition (i.e. under the three-edge loading condition) to the maximum positive bending moment in the field condition (obtained from the finite element modelling) as shown in Equation 6 (Young and O'Reilly, 1987; Petersen et al., 2010). The maximum bending moment in the laboratory condition (M_{lab}) can be found using Equation 2 (Young and O'Reilly, 1987). The total force applied on the pipe (W_t) in Equation 2 is the summation of the load due to backfill soil weight ($W_{backfill}$) and the traffic load ($W_{traffic}$) as shown in Equation 3 (BSI, 1997, BSI, 2010). The backfill soil weight ($W_{backfill}$) is calculated based on the BS (BSI, 1997, BSI, 2010), where the cases of narrow and wide trench should be compared and the minimum force should be considered as shown in Equation 4. Finally, the traffic load is calculated based on the BS using Equation 5 (BSI, 2010).

$$M_{lab} = W_t r \pi^{-1} \tag{2}$$

$$W_t = W_{backfill} + W_{traffic} \tag{3}$$

$$W_{backfill} = the\ minimum\ of\ (C_c \gamma D_{out}^2)\ and\ (C_d \gamma T_w^2) \tag{4}$$

$$W_{traffic} = \left(\frac{54.5}{H} + \frac{42}{1.8^H}\right) \times D_{out} \tag{5}$$

$$BF = \frac{M_{lab}}{M} \tag{6}$$

Where, r is the radius of the pipe measured to the centre of the pipe wall, C_c is the soil load factor for the case of wide trench condition, γ is the unit weight of the soil, D_{out} is the outside diameter of the pipe, C_d is the soil load factor for the case of a narrow trench condition, T_W is the trench width, H is the backfill height above the pipe and M is the maximum field bending moment predicted from the finite element modelling. Details of the calculation for determining the load coefficients C_c and C_d can be found in the BS (BSI, 1997, BSI, 2010).

Figure 10 shows the bedding factors obtained for the cases of good installation (SW90 soil in the haunch zone) (Figure 10 a) and poor installation (ML49 soil in the haunch zone) (Figure 10 b). Other installation conditions (haunch support with SW95 and ML90) have not been considered as the results of the parametric study showed an insignificant effect of these installation conditions on the bending moment comparing with the good installation (SW90 in the haunch zone). This means that these conditions will not significantly affect the bedding factor values.

It can be seen from Figure 10 that for the good installation condition, increasing the backfill height increases the bedding factor, whereas the relationship of the bedding factor with the backfill height for the poor installation condition depends on the pipe diameter. The difference in the trend behaviour of the bedding factor between the poor and good installation conditions is due to the independency of the laboratory force calculated following the BS method (Equations 4 and 5) on the installation condition, where Equations 4 and 5 assume that the maximum bending moment will always be at the pipe crown. Therefore, the laboratory bending moment will be the same for both installation conditions, while the field bending moment (obtained from the finite element modelling) is significantly affected by the support condition.

It can also be seen for both installation conditions that increasing the diameter of the pipe increases the bedding factor. This is due to the oversimplification in the design force calculation (Equations 4 and 5), where in Equations 4 and 5 the maximum vertical soil pressure at the pipe crown is multiplied by the pipe diameter to convert the soil pressure into a line load. This oversimplification leads to a very high value of the laboratory bending moment (M_{lab}) (Equation 2) as the diameter of the pipe increases, and hence provides a higher bedding factor value due to the significant increase of the laboratory bending moment term in the bedding factor equation (Equation 6).

The bedding factors obtained in this study were used to investigate the robustness of the design standard by calculating the ratio of the obtained bedding factor (BF(FEM)) to the design bedding factor (BF(BS)). The BS bedding factors were calculated using Table 1. A value of 1.9 was considered for the good installation condition, as it is similar to class B installation, and a value of 1.1 was considered for the poor installation condition, as the poor installation modelled in this paper is similar to class N and DD (i.e. where the pipe is installed directly on a stiff soil with poor support in the haunch zone).

Figure 11 shows the calculated ratio for pipes with wall thicknesses from Table 2, for good installation (Figure 11a) and poor installation (Figure 11b) conditions. It can be seen from the Figure that the BS bedding factors are overly conservative for both installation conditions, where the ratio of the obtained to design bedding factor ranges from 1.63 to 4.92 for the good installation and from 2.45 to 4.68 for the poor installation conditions. This is due to the oversimplification in the method used in the BS for calculating the force applied on the pipe, as mentioned in the previous section, where the BS method estimates the design force by multiplying the

maximum soil pressure at the crown of the pipe by the diameter of the pipe. This means that the BS method assumes the vertical soil pressure over the top half of the pipe will be equal to the maximum soil pressure at the pipe crown. However, the maximum vertical soil pressure over the top half of the pipe is significantly affected by the angle from the crown as shown in Figure 12. Figure 12 shows the total vertical pressure applied over the top half of pipes with a backfill height of 1.0 m buried in a good installation condition, calculated using the BS method and the finite element analyses. It can be seen from this Figure that although the BS method underestimates the maximum vertical soil pressure for all of the considered diameters, it also assumes a uniform soil pressure over the top half of the buried pipe. This assumption produces a very high design force and hence very high bending moments in the laboratory test. Furthermore, converting the force applied over the top half of the pipe to a line load and using this force in the laboratory test is not correct, especially for the good installation condition because this assumption concentrates all of the force in the pipe crown. However, the soil pressure in reality is applied over all of the top half of the pipe, including the crown and the shoulders of the pipe. Hence, it will affect all of the top half of the pipe and not only the crown. Therefore, it can be concluded that this methodology does not truly simulate the actual scenario and leads to an over conservative design.

As a result, a solution to these significant issues in the methodology of the load calculation is required to make sure that the design of the rigid buried pipes is robust and economic. However, any modified solution needs to be practical and related to the three-edge bearing test as this is the only available method to test the quality of the pipe. Thus, proposing new bedding factors based on the results of this study would improve the design methodology and implicitly account for the issues

demonstrated previously, hence enables a robust and economical design of concrete pipes. Attempts were therefore made to use the non-linear regression analysis approach to fit the bedding factors obtained in this study and propose equations for determining the bedding factors. However, these attempts provided equations with poor accuracy. Consequently, an advanced data mining technique called Evolutionary Polynomial Regression (EPR) was employed to derive explicit and concise mathematical models for the bedding factors. This technique was chosen since is it has been successfully used by other researchers to model complex relationships (Alzabeebee et al., 2018; Ahangar Asr and Javadi, 2016; Alani et al., 2014; Faramarzi et al., 2014; Faramarzi et al., 2013; Faramarzi et al., 2012; Javadi et al., 2012; Savic et al., 2006). The EPR methodology and the development of the bedding factor models are discussed in the next section.

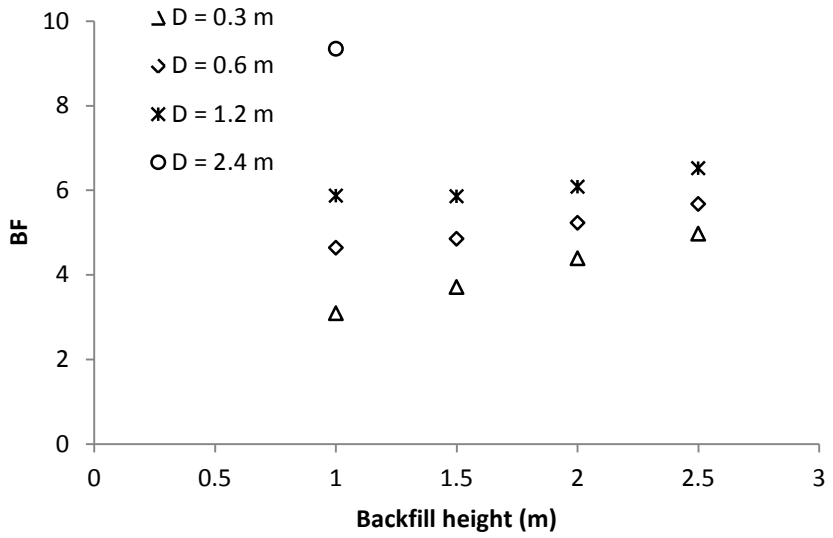

(a)

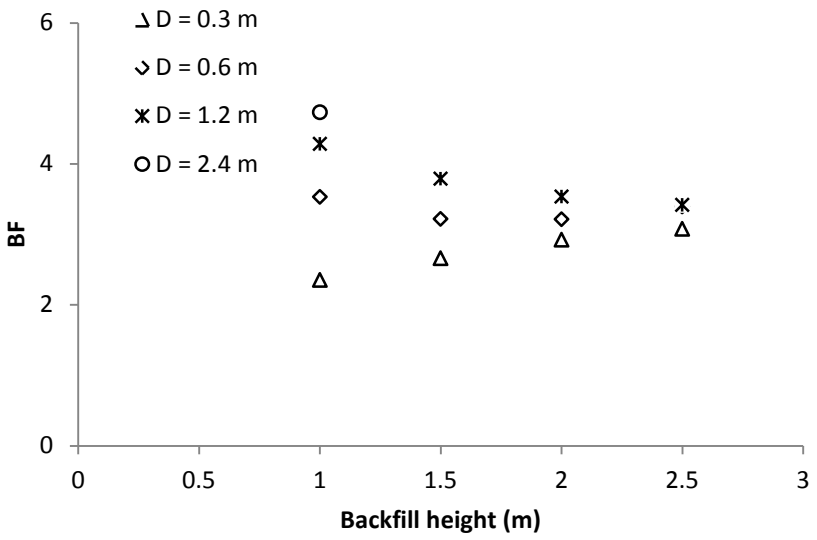

(b)

Figure 10: Calculated bedding factor for pipes with sizes as in Table 2: (a) good installation (SW90 soil in the haunch zone); (b) poor installation (ML49 soil in the haunch zone)

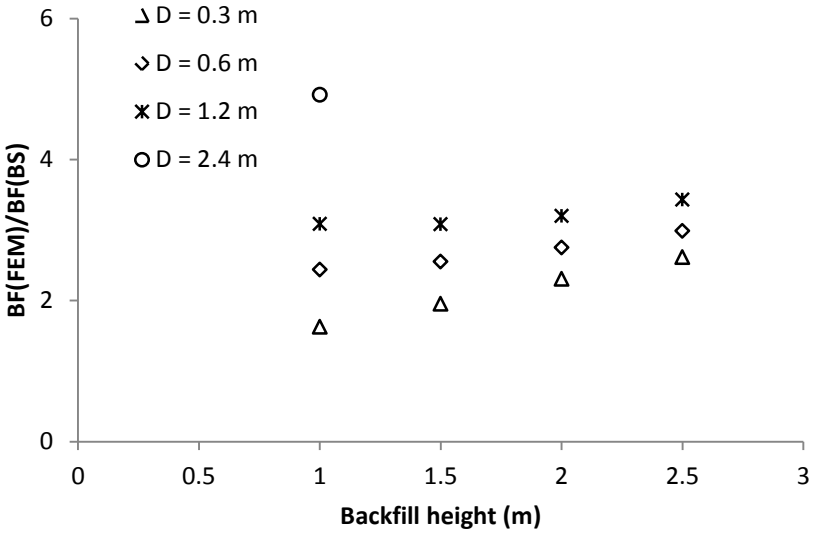

(a)

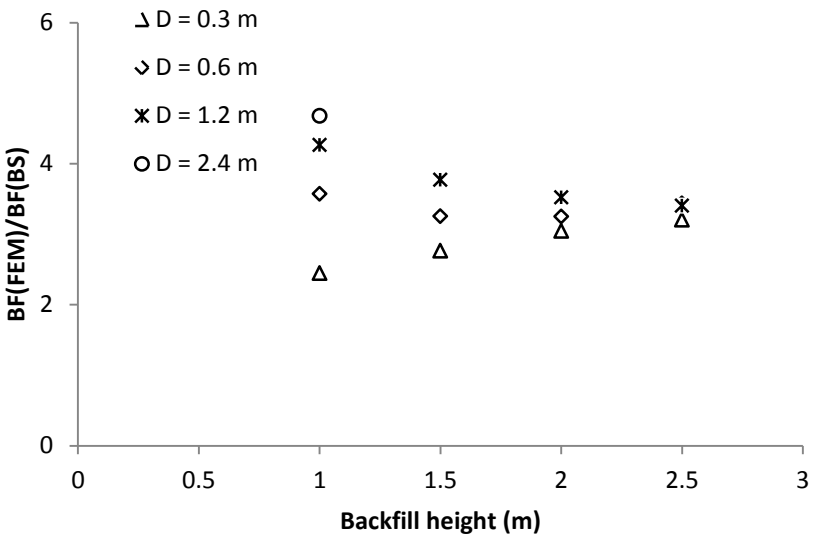

(b)

Figure 11: Ratio of bedding factors obtained from the numerical modelling and the BS values: (a) good installation; (b) poor installation

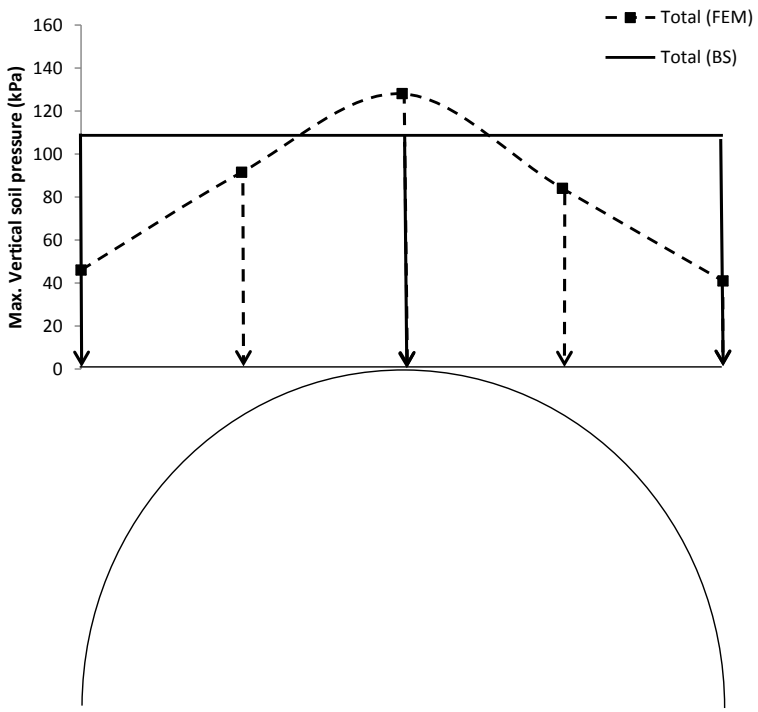

(a)

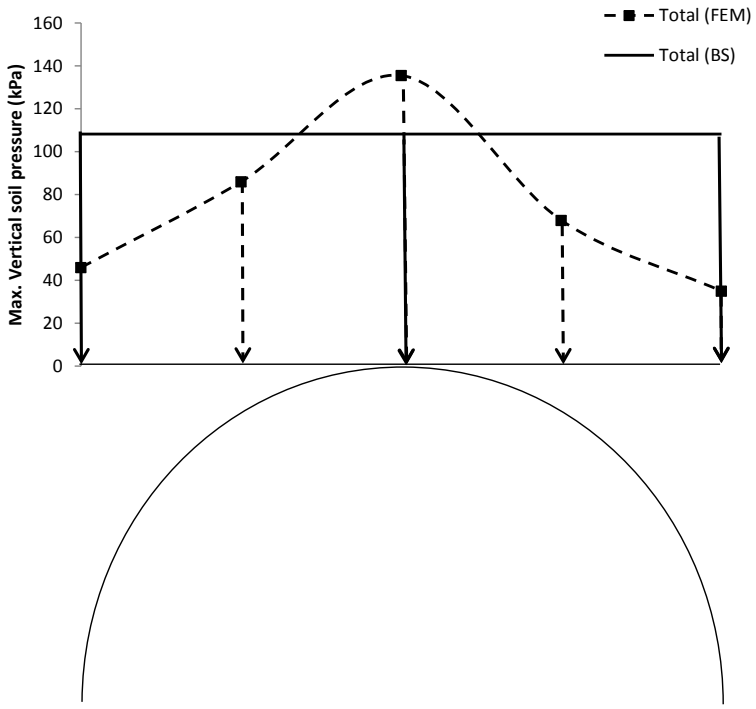
Total (FEM)
Total (BS)
Max. Vertical soil pressure (kPa)
160
140
120
100
80
60
40
20
0

(b)

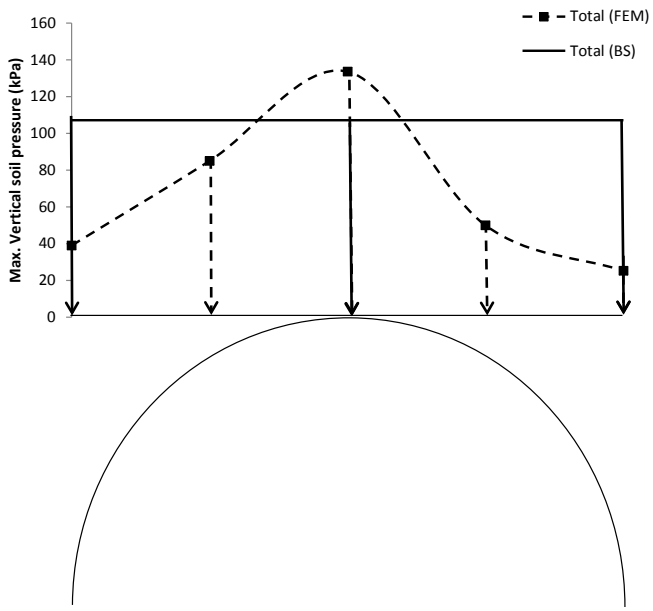
Total (FEM)
Total (BS)
Max. Vertical soil pressure (kPa)
160
140
120
100
80
60
40
20
0

(c)

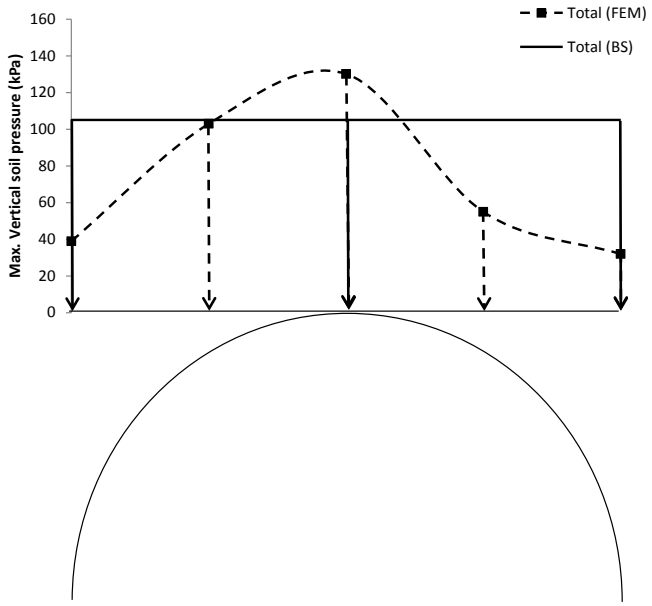

(d)

Figure 12: The BS and finite element analysis results of the total maximum vertical soil pressure applied over the top half of the pipes buried in the good installation condition with a backfill height of 1.0 m: (a) D = 0.3 m; (b) D = 0.6 m; (c) D = 1.2 m; (d) D = 2.4 m

6. Development of the model

6.1. The EPR method

Evolutionary Polynomial Regression (EPR) is a data mining method that combines the least square fitting technique with the genetic algorithm optimisation to find the best mathematical expression that describes the relationship between the input and output data (Giustolisi and Savic, 2006). The EPR method starts from Equation 7 (Giustolisi and Savic, 2006).

$$y = \sum_{j=1}^{m} F\left(\mathbf{X}, f(\mathbf{X}), a_j\right) + a_0 \quad (7)$$

Where y is the estimated output of the system, a_j is a constant value, F is a function evolved during the process depending on the input and output data, $\boldsymbol{X}$ is the matrix of the input independent variables, f is the type of function defined by the user and m is the number of terms in the proposed model excluding the bias term a_0.

The least square fitting technique is used to solve the overdetermined system in Equation 7 (Giustolisi and Savic, 2006) and a genetic algorithm is used to find the best fit mathematical expression by changing the order of the exponents based on the range specified initially (further details can be found in Giustolisi and Savic, 2006). The coefficient of determination (CD) (Equation 8) is calculated for each relationship, where the relationship which achieves the highest CD value is selected (Alani et al., 2014; Faramarzi et al., 2014).

$$CD = 1 - \frac{\sum_N (Y_a - Y_p)^2}{\sum_N \left(Y_a - \frac{1}{N}\sum_N Y_p\right)^2} \quad (8)$$

Where Y_a is the dependent input value, Y_p is the predicted dependent input value from the EPR model and N is the number of the data points.

Giustolisi and Savic (2006) developed the original EPR procedure with a single-objective, where the fitness of the mathematical expression was selected based on the best fit model with a penalisation technique to avoid overfitting the problem (Giustolisi and Savic, 2006). However, Giustolisi and Savic (2009) improved this technique and developed a multi-objective EPR (EPR-MOGA) because the single objective EPR had a number of disadvantages. The improvement involved utilising one objective to control the fitness of the model, while the complexity of the model is controlled by using one or two functions. Therefore, the present analysis utilises the

multi-objective EPR. Further details about the EPR-MOGA technique can be found in (Giustolisi and Savic, 2009).

6.2. Modelling the bedding factor

The results of the parametric study showed that the bedding factor is significantly affected by the pipe diameter, pipe wall thickness and backfill height. Therefore, incorporating all of these parameters is necessary to ensure that the developed models are robust and representative. Hence, all of the bedding factor data were used to develop the bedding factor model for each installation condition (i.e. good and poor installation conditions). The data are divided into training data (80%) and validation data (20%). This process is used in the EPR modelling technique because it is not a simple curve fitting method, as the EPR searches for the best model using a training methodology. Therefore, the developed model should be tested using unseen data to ensure that the model is reliable and able to predict the trend behaviour. Furthermore, the general statistical characteristics of the training and validation data should be similar to avoid model extrapolation (Alani et al., 2014). Therefore, an effort was made to carefully divide the data into training and validation data sets with comparable general statistical characteristics. Table 4 shows the standard deviation (STDV), maximum (Max), minimum (Min) and mean (mean) values for the data used for the training, validation and all the data used in the modelling for both the good and poor installation conditions.

Several attempts were made to obtain a mathematical expression with a very high accuracy by trying different exponents for the developed mathematical expression, different function types and different number of terms. In every attempt, the EPR changes the exponent of the independent parameters based on the genetic algorithm and the range specified initially, solves the mathematical system using the

least squares method and finally calculates the coefficient of determination (CD) (Equation 8). As the number of iterations increases, the EPR learns the best exponent arrangement. Subsequently, the EPR increases the number of terms and repeats the aforementioned procedure until it reaches the maximum number of terms. Ultimately, the EPR reports the final models with the CD value for the training and validation data. It was found that as the number of terms increases, the CD value also increases. However, increasing the number of terms increases the model complexity and increases the possibility of overfitting. Therefore, the selection of the models was done based on the model simplicity and the ability of the model to represent the trend behaviour of the input data. The ability to replicate the trend behaviour was checked by carefully comparing the results of the developed models with the original data. The simplest model, which was able to reasonably replicate the trend was selected for each installation condition. Equations 9 and 10 show the selected models for the good and poor installation conditions, respectively.

$$BF = -0.21\frac{1}{\sqrt{D}\sqrt{t}} + 6.15\frac{\sqrt{t}\sqrt{H}}{\sqrt{D}} + 0.017\frac{D^2\sqrt{H}}{t^2} + 0.35\frac{D^2}{\sqrt{t}H^2} + 1.52 \quad (9)$$

$$\mathrm{BF} = -0.13\frac{1}{\sqrt{\mathrm{t}}\mathrm{DH}^2} + 9\frac{\mathrm{t}}{\mathrm{D}} + 0.15\frac{\mathrm{D}}{\mathrm{t\,H}^2} + 0.007\frac{\mathrm{D}^2}{\mathrm{t}^2} + 1.55 \quad (10)$$

Figures 13 a and b compare the finite element results with the EPR model results for both the training and validation data. Furthermore, Table 5 presents the CD value for the training and validation data for both models. Figure 13, together with Table 5, illustrate that the models developed using this procedure are able to predict the bedding factor with a very high accuracy.

It should be noted that the dimensions of the independent variables (the pipe inside diameter (D), pipe wall thickness (t) and backfill height (H)) should have the unit of metres for the correct prediction of the bedding factor from Equations 9 and 10, as this unit was used to derive these empirical models. In these equations, the bedding factor is a dimensionless parameter and the coefficients used in these formulas have appropriate units to achieve this. Furthermore, it is important to mention that the bedding factors are derived using the field bending moment (obtained from the numerical modelling). When considering the normal procedure for the design of buried concrete pipes, the bedding factor is used to find the required crushing strength of the pipe. This crushing strength corresponds to a crack width of 0.254 mm. Hence, the field bending moment will correspond to a crack width value of 0.254 mm. In other words, the derived bedding factors correspond to a crack width of 0.254 mm or to a crack width considered appropriate by the designer in the three-edge bearing test, if he/she considers a crack width different from the design standard.

Table 4: Statistics for the data used in the EPR analysis

		Good installation				Poor installation			
		D (m)	t (m)	H (m)	BF	D (m)	t (m)	H (m)	BF
Training data	Mean	0.81	0.11	1.66	6.63	0.81	0.10	1.72	4.07
	Min	0.30	0.03	1.00	3.09	0.30	0.03	1.00	2.35
	Max	2.40	0.46	2.50	16.38	2.40	0.46	2.50	8.06
	STDV	0.57	0.09	0.58	2.77	0.56	0.09	0.59	1.17
Validation data	Mean	0.90	0.12	1.81	6.50	0.94	0.15	1.57	3.49
	Min	0.30	0.03	1.00	3.36	0.30	0.03	1.00	2.44
	Max	2.40	0.25	2.50	13.07	2.40	0.25	2.50	4.73
	STDV	0.70	0.09	0.59	3.21	0.74	0.10	0.53	0.80
All data	Mean	0.83	0.11	1.69	6.60	0.83	0.11	1.69	3.96
	Min	0.30	0.03	1.00	3.09	0.30	0.03	1.00	2.35
	Max	2.40	0.46	2.50	16.38	2.40	0.46	2.50	8.06
	STDV	0.59	0.09	0.58	2.82	0.59	0.09	0.58	1.13

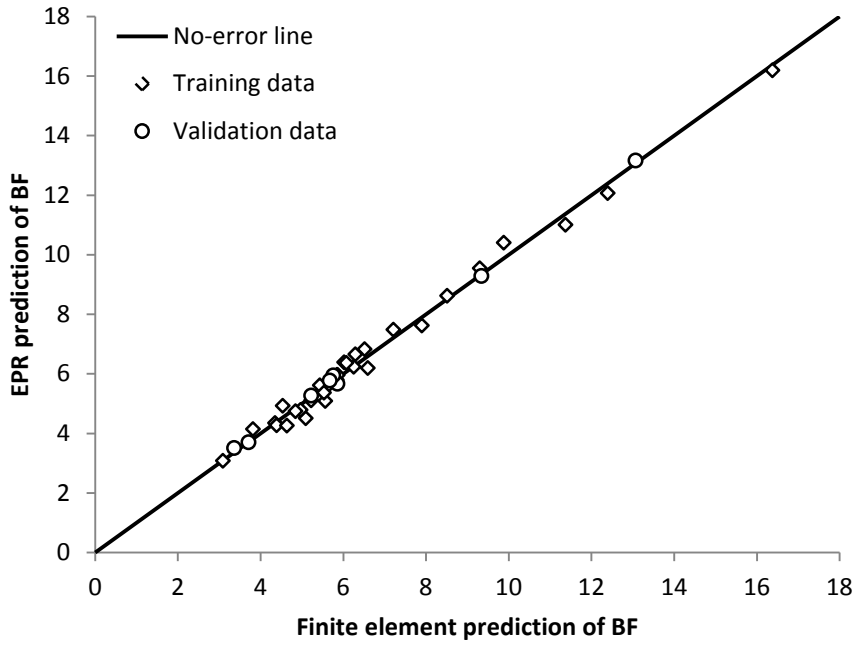

(a)

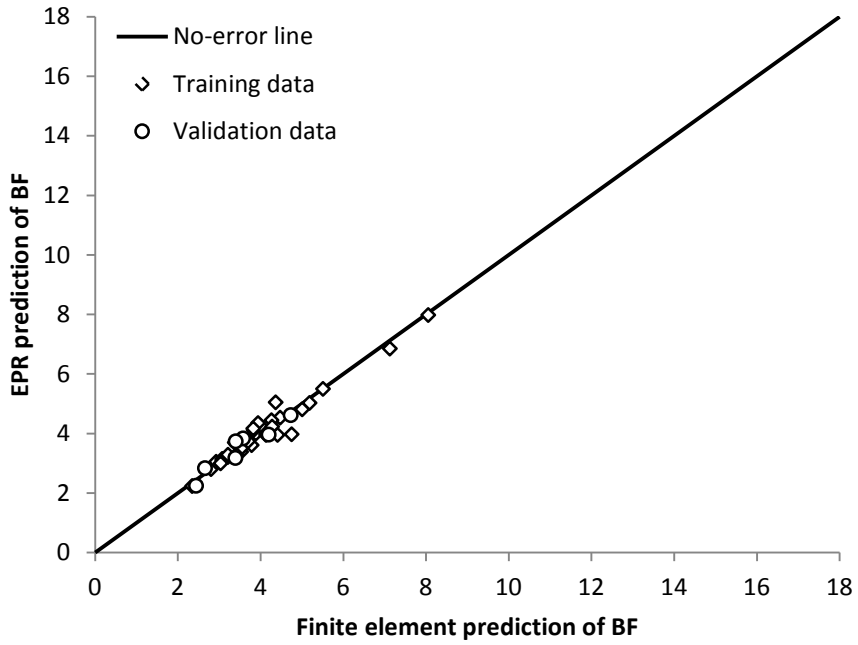

(b)

Figure 13: EPR predicted bedding factors compared to the finite element results: (a) good installation; (b) poor installation

Table 5: Coefficient of determination (CD) for the training and validation data (%)

Data set	Good installation	Poor installation
Training	98.97	94.41
Validation	99.41	89.64

6.3. Sensitivity analysis

A sensitivity analysis has been conducted by comparing the trend behaviour of the developed models with that discussed in section 5 in order to develop additional confidence in the predictive ability of these models. Figures14 a and b show the results of the comparison of the calculated (using finite element modelling) and predicted (using EPR) bedding factor values for all of the considered diameters and backfill heights for both the good (Equation 9) (Figure 14 a) and poor installation conditions (Equation 10) (Figure 14 b). It can be seen from Figure 14 a that the developed model for the good installation is able to predict the trend behaviour observed and discussed in section 5, where increasing the pipe diameter and the backfill height increase the bedding factor. Figure 14 b shows that the developed model for the poor installation is able to model the dependency of the bedding factor-backfill height relationship on the pipe diameter. Hence, these models can be used with confidence to overcome the oversimplifications in the design standard and ensure robust and economical designs. It should be noted, however, these models have been derived and tested using pipes with an inside diameter range of 0.3 m to 2.4 m. Therefore, the use of these models for predicting the bedding factor of pipes outside this diameter range is not recommended and may cause significant errors.

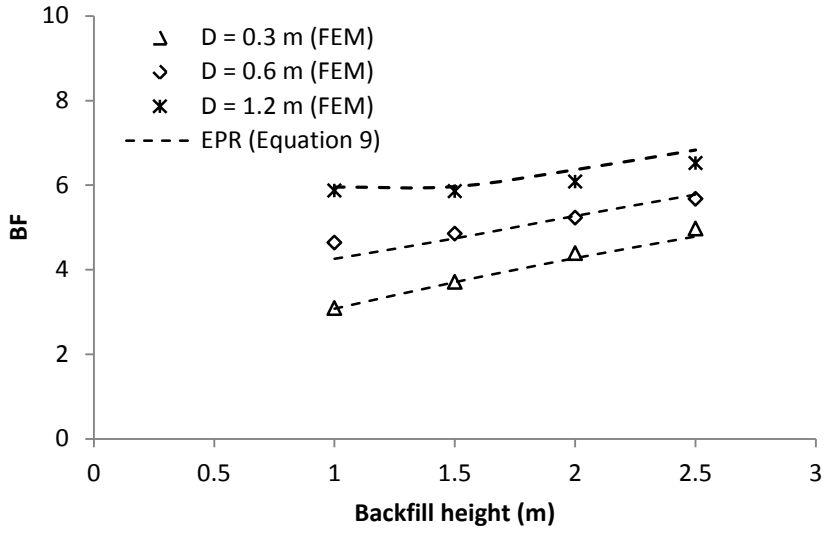

(a)

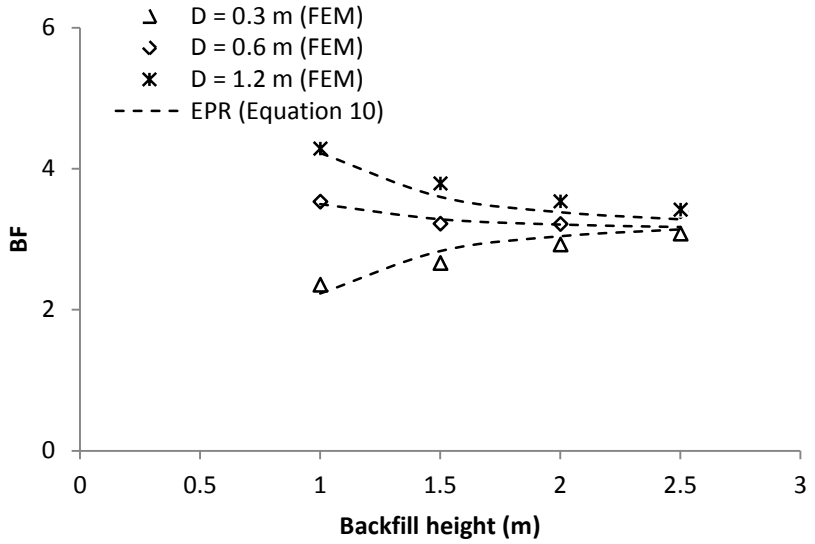

(b)

Figure 14: The results of the sensitivity analysis for the pipe diameters shown in Table 2: (a) good installation; (b) poor installation

Conclusions

This paper has investigated the response of buried concrete pipes with inside diameters ranging from 0.3 m to 2.4 m under the BS main highway (‘main road’) traffic load requirements, using a validated three-dimensional finite element model. The study provided an insight into the effect of the pipe diameter and backfill height on both the developed bending moment in the pipe wall and the soil pressure around the pipe. Furthermore, this study has presented for the first time a rigorous investigation into the robustness of the British Standard methodology for designing buried concrete pipes. The following conclusions can be drawn from the present study:

1- The effect of traffic load is significantly affected by the pipe diameter, where increasing the diameter of the pipe decreases the influence of the traffic load. However, the traffic load does not affect the developed bending moment in the pipe wall for a backfill height of greater than 2.5 m for pipes with an inside diameter of 0.3 to 1.2 m. Moreover, the effect of traffic load vanishes after a backfill height of 1.0 m for a pipe with an inside diameter of 2.4 m. Therefore, the study suggests including these backfill height limits to the effect of the traffic load.

2- The developed bending moment in the pipe wall is significantly affected by the pipe wall thickness, where increasing the pipe thickness increases the bending moment.

3- Changing the support condition from a very good installation (using SW95 soil in the haunch zone) to a reasonable installation (using ML90 soil in the haunch zone) does not significantly affect the developed bending moment. However, providing a poor support condition for the pipe in the haunch zone significantly

increases the bending moment. Hence, a better pipe performance can be achieved by providing a good support in the haunch zone.

4- The results showed that the British Standard method to calculate the force applied on the pipe is overly conservative, where the assumption of a uniform vertical soil pressure above the top half of the pipe with a magnitude equal to the vertical soil pressure at the pipe crown does not represent the real condition. This assumption leads to a very high design load, and hence an uneconomical design.

5- The calculated bedding factors based on the results of the finite element modelling showed that the bedding factors adopted in the British Standard are overly conservative, where the ratio of the predicted to the obtained bedding factors ranging from 1.63 to 4.92. The study illustrated that this over conservatism is due the oversimplification in the design force calculation based on the British Standard.

6- New bedding factor models have been proposed using the evolutionary polynomial regression analysis technique for both the good and poor installation conditions. The use of these models ensures an economical and robust design of concrete pipes as these models implicitly account to the error due to the oversimplification in the force calculation following the BS method.

Acknowledgment

The first author thanks the financial support for his PhD study provided by the higher committee for education development in Iraq (HCED).

References

ACPA (American Concrete Pipe Association) (2011) Concrete pipe design manual. American Concrete Pipe Association. See http://www.concrete pipe.org/pages/design-manual.htm (accessed 24/09/2015).

Ahangar Asr, A. and Javadi, A., 2016. Air losses in compressed air tunnelling: a prediction model. Proceedings of the Institution of Civil Engineers-Engineering and Computational Mechanics, 169(3), 140-147

Alani, A.M., Faramarzi, A., Mahmoodian, M., Tee, K.F. (2014). Prediction of sulphide build-up in filled sewer pipes. Environmental Technology, 35(14), 1721-1728.

Allard, E., El Naggar, H., 2016. Pressure distribution around rigid culverts considering soil-structure interaction effects. International Journal of Geomechanics, 16(2), 04015056.

Alzabeebee, S., Chapman, D., Jefferson, I. and Faramarzi, A., 2017a. The response of buried pipes to UK standard traffic loading. Proceedings of the Institution of Civil Engineers-Geotechnical Engineering, 170(1), 38-50.

Alzabeebee, S., Chapman, D.N. and Faramarzi, A., 2017b, Numerical investigation of the bedding factor of concrete pipes under deep soil fill. In the Proceedings of the 2nd World Congress on Civil, Structural, and Environmental Engineering (CSEE'17) Barcelona, Spain, paper number 119.

Alzabeebee, S., Chapman, D.N., Faramarzi, A., 2018. Development of a novel model to estimate bedding factors to ensure the economic and robust design of rigid pipes under soil loads, Tunneling and Underground Space Technology, 71, 567-578.

Alzabeebee, S., Chapman, D.N., Jefferson and I. Faramarzi, A., 2016. Investigating the maximum soil pressure on a concrete pipe with poor haunch support subjected to traffic live load using numerical modelling. 11th Pipeline Technology Conference Berlin, Germany, 11 pages.

Arockiasamy, M., Chaallal, O., Limpeteeprakarn, T., 2006. Full-scale field tests on flexible pipes under live load application. Journal of Performance of Constructed Facilities 20 (1), 21–27.

Ban, H., Park, S. W., Kim, Y. R., 2013. Performance evaluation of buried concrete pipe under heavy traffic load. Journal of the Korean Geotechnical Society 29 (12), 69-75. (In Korean).

Boscardin, M.D., Selig, E.T., Lin, R.S., Yang, G.R., 1990. Hyperbolic parameter for compacted soils. Journal of Geotechnical Engineering ASCE 116 (1), 88–104.

Brown, S.F., and Selig, E.T., 1991. The design of pavement and rail track foundations. In: O'Reilly M.P., Brown, S.F. (Eds.) Cyclic loading of soils: from theory to practice. Blackie and Son Ltd, Glasgow and London, U.K., pp. 249-305.

BS 9295, 2010. Guide to the structural design of buried pipelines. BSI, London, UK.

BS EN 1295-1, 1997. Structural design of buried pipelines under various conditions of loading – part 1: general requirements. BSI, London.

Dhar, A.S., Moore, I.D., McGrath, T.J., 2004. Two-dimensional analyses of thermoplastic culvert displacements and strains. Journal of Geotechnical and Geoenvironmental Engineering 130 (2), 199–208.

Duncan, J.M., Chang, C., 1970. Nonlinear analysis of stress and strain in soils. Journal of the Soil Mechanics and Foundations Division ASCE 96 (5), 1629–1653.

El Naggar, H., Turan, A., Valsangkar, A., 2015. Earth pressure reduction system using geogrid-reinforced platform bridging for buried utilities. Journal of Geotechnical and Geoenvironmental Engineering, 141(6), 04015024.

Faramarzi, A, Javadi, A.A., Alani, A.M. (2012). EPR-based material modelling of soils considering volume changes. Computers and Geosciences, 48, 73-85.

Faramarzi, A., Alani, A.M., Javadi, A.A. (2014). An EPR-based self-learning approach to material modelling. Computers and Structures 137, 63-71.

Faramarzi, A., Javadi, A.A., Ahangar-Asr, A. (2013). Numerical implementation of EPR-based material models in finite element analysis. Computers and Structures, 118, 100-108.

Giustolisi, O., Savic, D.A., 2006. A symbolic data-driven technique based on evolutionary polynomial regression. Journal of Hydroinformatics, 8(3), 207-222.

Giustolisi, O., Savic, D.A., 2009. Advances in data-driven analyses and modelling using EPR-MOGA. Journal of Hydroinformatics, 11(3-4), 225-236.

HA (Highways Agency) (2001) Design Manual for Roads and Bridges – Volume 4, Section 2, Part 5: HA 40/01: Determination of Pipe and Bedding Combination for Drainage Work. The Stationery Office, London, UK.

Javadi, A.A., Faramarzi, A., Ahangar-Asr, A. (2012). Analysis of behaviour of soils under cyclic loading using EPR-based finite element method. Finite Elements in Analysis and Design, 58, 53-65.

Kang, J., Jung, Y., Ahn, Y., 2013a. Cover requirements of thermoplastic pipes used under highways. Composites Part B-Engineering 55, 184-192.

Kang, J., Parker, F., Yoo, C.H., 2007. Soil-structure interaction and imperfect trench installation for deeply buried concrete pipes. Journal of Geotechnical and Geoenvironmental Engineering 133 (3), 277–285.

Kang, J., Parker, F., Yoo, C.H., 2008a. Soil–structure interaction for deeply buried corrugated steel pipes Part I: Embankment installation. Engineering Structures, 30(2), 384-392.

Kang, J., Parker, F., Yoo, C.H., 2008b. Soil–structure interaction for deeply buried corrugated steel pipes Part II: Imperfect trench installation. Engineering Structures, 30(3), 588-594.

Kang, J., Stuart, S.J., Davidson, J.S., 2014. Analytical study of minimum cover required for thermoplastic pipes used in highway construction. Structure and Infrastructure Engineering 10(3), 316-327.

Kang, J.S., Stuart, S.J., Davidson, J.S., 2013b. Analytical evaluation of maximum cover limits for thermoplastic pipes used in highway construction. Structure and Infrastructure Engineering 9(7), 667-674.

Katona, M.G., 2017. Influence of Soil Models on Structural Performance of Buried Culverts. International Journal of Geomechanics, 17 (1), 04016031.

Kim, K., Yoo, C.H., 2005. Design loading on deeply buried box culverts. Journal of Geotechnical and Geoenvironmental Engineering 131(1), 20-27.

Lay, G.R., Brachman, R.W.I., 2014. Full-scale physical testing of a buried reinforced concrete pipe under axle load. Canadian Geotechnical Journal 51 (4), 394–408.

MacDougall, K., Hoult, N. A., Moore, I.D., 2016. Measured load capacity of buried reinforced concrete pipes. ACI Structural Journal 113 (1), 63-73.

Mehrjardi, G.T., Tafreshi, S.N.M., Dawson, A.R., 2015. Numerical analysis on buried pipes protected by combination of geocell reinforcement and rubber-soil mixture. International Journal of Civil Engineering 13(2), 90-104.

Mohamed, N., Soliman, A.M., Nehdi, M.L., 2014. Full-scale pipes using dry-cast steel fibre-reinforced concrete. Construction and Building Materials, 72, 411-422.

Moore, I.D., 2001. Buried pipes and culverts. In: Rowe, R.K. (Ed.), Geotechnical and Geoenvironmental Engineering Handbook. Kluwer Academic Publishing, Norwell, U.S.A, pp. 539‑566.

Moore, I.D., Hoult, N.A. and MacDougall, K. (2014) Establishment of Appropriate Guidelines for Use of the Direct and Indirect Design Methods for Reinforced Concrete Pipe, Contractor's Final Report for NCHRP Project 20-07 Task 316, March 2014 National Cooperative Highway Research Program, National Academy of Sciences Transportation Research Board, Washington D.C.126 pp.

Nehdi, M. L., Mohamed, N., Soliman, A. M., 2016. Investigation of buried full-scale SFRC pipes under live loads. Construction and Building Materials 102, 733-742.

Petersen, D.L., Nelson, C.R., Li, G., McGrath, T.J., Kitane, Y., 2010. NCHTP Report 647: Recommended Design Specifications for Live Load Distribution to Buried Structures. Transportation Research Board, Washington D.C..

Pettibone, H.C., Howard, A.K., 1967. Distribution of soil pressures on concrete pipe. Journal of the pipeline division 93 (2), 85-102.

Rakitin, B., Xu, M., 2014. Centrifuge modeling of large-diameter underground pipes subjected to heavy traffic loads. Canadian Geotechnical Journal 51 (4), 353–368.

Savic, D., Giustolisi, O., Berardi, L., Shepherd, W., Djordjevic, S., and Saul, A. (2006). Modelling sewer failure by evolutionary computing. Proceedings of the Institution of Civil Engineers - Water Management, 159(2), 111-118.

Turan, A., El Nagger, M.H., Dundas, D., 2013. Investigation of induced trench method using a full scale test embankment. Geotechnical and Geological Engineering 31 (2), 557-568.

Wong, L.S., Allouche, E.N., Dhar, A.S., Baumert, M., Moore, I.D., 2006. Long-term monitoring of SIDD type IV installations. Canadian Geotechnical Journal 43(4), 392-408.

Young, O.C., O'Reilly, M.P. 1987. A guide to design loadings for buried rigid pipes. Transport and Road Research Laboratory, Department of Transport. London: HMSO, 1983, Second Impression 1987.